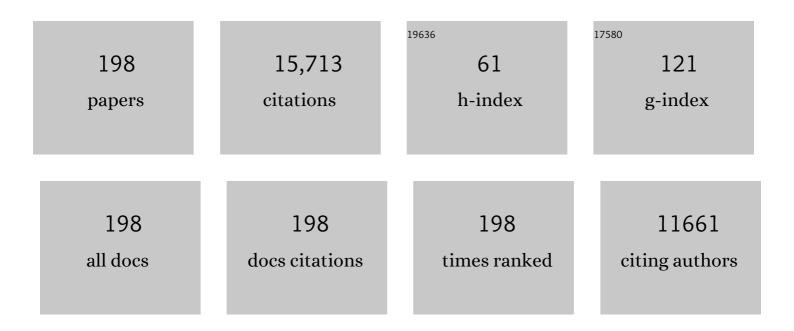
Xin-Bing Zhao

List of Publications by Year in descending order

Source: https://exaly.com/author-pdf/524867/publications.pdf Version: 2024-02-01



#	Article	IF	CITATIONS
1	Compromise and Synergy in Highâ€Efficiency Thermoelectric Materials. Advanced Materials, 2017, 29, 1605884.	11.1	1,098
2	Realizing high figure of merit in heavy-band p-type half-Heusler thermoelectric materials. Nature Communications, 2015, 6, 8144.	5.8	893
3	Self-supported hydrothermal synthesized hollow Co3O4 nanowire arrays with high supercapacitor capacitance. Journal of Materials Chemistry, 2011, 21, 9319.	6.7	669
4	Point Defect Engineering of Highâ€Performance Bismuthâ€Tellurideâ€Based Thermoelectric Materials. Advanced Functional Materials, 2014, 24, 5211-5218.	7.8	619
5	Band engineering of high performance p-type FeNbSb based half-Heusler thermoelectric materials for figure of merit zT > 1. Energy and Environmental Science, 2015, 8, 216-220.	15.6	469
6	Freestanding Co3O4 nanowire array for high performance supercapacitors. RSC Advances, 2012, 2, 1835.	1.7	414
7	Few‣ayered SnS ₂ on Few‣ayered Reduced Graphene Oxide as Na″on Battery Anode with Ultralong Cycle Life and Superior Rate Capability. Advanced Functional Materials, 2015, 25, 481-489.	7.8	391
8	High Efficiency Halfâ€Heusler Thermoelectric Materials for Energy Harvesting. Advanced Energy Materials, 2015, 5, 1500588.	10.2	380
9	Tuning Multiscale Microstructures to Enhance Thermoelectric Performance of nâ€Type Bismuthâ€Tellurideâ€Based Solid Solutions. Advanced Energy Materials, 2015, 5, 1500411.	10.2	379
10	High-performance half-Heusler thermoelectric materials Hf1â^'x ZrxNiSn1â^'ySby prepared by levitation melting and spark plasma sintering. Acta Materialia, 2009, 57, 2757-2764.	3.8	373
11	Beneficial Contribution of Alloy Disorder to Electron and Phonon Transport in Halfâ€Heusler Thermoelectric Materials. Advanced Functional Materials, 2013, 23, 5123-5130.	7.8	349
12	Single-Crystalline LiMn2O4 Nanotubes Synthesized Via Template-Engaged Reaction as Cathodes for High-Power Lithium Ion Batteries. Advanced Functional Materials, 2011, 21, 348-355.	7.8	327
13	New Insights into Intrinsic Point Defects in V ₂ VI ₃ Thermoelectric Materials. Advanced Science, 2016, 3, 1600004.	5.6	317
14	Hierarchically porous NiO film grown by chemical bath depositionvia a colloidal crystal template as an electrochemical pseudocapacitor material. Journal of Materials Chemistry, 2011, 21, 671-679.	6.7	282
15	Smallest Carbon Nanotube Is3  Åin Diameter. Physical Review Letters, 2004, 92, 125502.	2.9	272
16	Shifting up the optimum figure of merit of p-type bismuth telluride-based thermoelectric materials for power generation by suppressing intrinsic conduction. NPG Asia Materials, 2014, 6, e88-e88.	3.8	272
17	High Band Degeneracy Contributes to High Thermoelectric Performance in pâ€Type Halfâ€Heusler Compounds. Advanced Energy Materials, 2014, 4, 1400600.	10.2	261
18	Low Electron Scattering Potentials in High Performance Mg ₂ Si _{0.45} Sn _{0.55} Based Thermoelectric Solid Solutions with Band Convergence. Advanced Energy Materials, 2013, 3, 1238-1244.	10.2	220

#	Article	IF	CITATIONS
19	The intrinsic disorder related alloy scattering in ZrNiSn half-Heusler thermoelectric materials. Scientific Reports, 2014, 4, 6888.	1.6	213
20	Hierarchical Chemical Bonds Contributing to the Intrinsically Low Thermal Conductivity in αâ€MgAgSb Thermoelectric Materials. Advanced Functional Materials, 2017, 27, 1604145.	7.8	195
21	Unique Role of Refractory Ta Alloying in Enhancing the Figure of Merit of NbFeSb Thermoelectric Materials. Advanced Energy Materials, 2018, 8, 1701313.	10.2	181
22	Recrystallization induced in situ nanostructures in bulk bismuth antimony tellurides: a simple top down route and improved thermoelectric properties. Energy and Environmental Science, 2010, 3, 1519.	15.6	174
23	Flexible carbon nanotube papers with improved thermoelectric properties. Energy and Environmental Science, 2012, 5, 5364-5369.	15.6	164
24	Nitrogen-doped reduced graphene oxide for high-performance flexible all-solid-state micro-supercapacitors. Journal of Materials Chemistry A, 2014, 2, 18125-18131.	5.2	158
25	Direct Growth of Flowerâ€Like Î′â€MnO ₂ on Threeâ€Dimensional Graphene for Highâ€Performance Rechargeable Liâ€O ₂ Batteries. Advanced Energy Materials, 2014, 4, 1301960.	10.2	154
26	Enhancing the Figure of Merit of Heavyâ€Band Thermoelectric Materials Through Hierarchical Phonon Scattering. Advanced Science, 2016, 3, 1600035.	5.6	147
27	Carrier grain boundary scattering in thermoelectric materials. Energy and Environmental Science, 2022, 15, 1406-1422.	15.6	145
28	High Performance Mg ₂ (Si,Sn) Solid Solutions: a Point Defect Chemistry Approach to Enhancing Thermoelectric Properties. Advanced Functional Materials, 2014, 24, 3776-3781.	7.8	141
29	Demonstration of a phonon-glass electron-crystal strategy in (Hf,Zr)NiSn half-Heusler thermoelectric materials by alloying. Journal of Materials Chemistry A, 2015, 3, 22716-22722.	5.2	137
30	Complex Band Structures and Lattice Dynamics of Bi ₂ Te ₃ â€Based Compounds and Solid Solutions. Advanced Functional Materials, 2019, 29, 1900677.	7.8	135
31	Biodegradable Magnesium Alloys Developed as Bone Repair Materials: A Review. Scanning, 2018, 2018, 1-15.	0.7	134
32	Multiple Converged Conduction Bands in K ₂ Bi ₈ Se ₁₃ : A Promising Thermoelectric Material with Extremely Low Thermal Conductivity. Journal of the American Chemical Society, 2016, 138, 16364-16371.	6.6	130
33	High Performance α-MgAgSb Thermoelectric Materials for Low Temperature Power Generation. Chemistry of Materials, 2015, 27, 909-913.	3.2	124
34	Enhanced Thermoelectric Performance in 18 lectron Nb _{0.8} CoSb Halfâ€Heusler Compound with Intrinsic Nb Vacancies. Advanced Functional Materials, 2018, 28, 1705845.	7.8	124
35	Self-assembly of a CoFe2O4/graphene sandwich by a controllable and general route: towards a high-performance anode for Li-ion batteries. Journal of Materials Chemistry, 2012, 22, 19738.	6.7	122
36	Attaining high mid-temperature performance in (Bi,Sb)2Te3 thermoelectric materials via synergistic optimization. NPG Asia Materials, 2016, 8, e302-e302.	3.8	119

#	Article	IF	CITATIONS
37	Enhanced thermoelectric performance of PbTe bulk materials with figure of merit zT >2 by multi-functional alloying. Journal of Materiomics, 2016, 2, 141-149.	2.8	118
38	Mg vacancy and dislocation strains as strong phonon scatterers in Mg 2 Si 1â^'x Sb x thermoelectric materials. Nano Energy, 2017, 34, 428-436.	8.2	116
39	Enhancement in thermoelectric performance of bismuth telluride based alloys by multi-scale microstructural effects. Journal of Materials Chemistry, 2012, 22, 16484.	6.7	110
40	Hot deformation induced bulk nanostructuring of unidirectionally grown p-type (Bi,Sb)2Te3 thermoelectric materials. Journal of Materials Chemistry A, 2013, 1, 11589.	5.2	110
41	Enhanced thermoelectric properties of p-type CoSb3/graphene nanocomposite. Journal of Materials Chemistry A, 2013, 1, 13111.	5.2	109
42	Roles of interstitial Mg in improving thermoelectric properties of Sb-doped Mg2Si0.4Sn0.6 solid solutions. Journal of Materials Chemistry, 2012, 22, 6838.	6.7	107
43	Valleytronics in thermoelectric materials. Npj Quantum Materials, 2018, 3, .	1.8	104
44	Lanthanide Contraction as a Design Factor for Highâ€Performance Halfâ€Heusler Thermoelectric Materials. Advanced Materials, 2018, 30, e1800881.	11.1	101
45	Flux synthesis and thermoelectric properties of eco-friendly Sb doped Mg2Si0.5Sn0.5 solid solutions for energy harvesting. Journal of Materials Chemistry, 2011, 21, 5933.	6.7	96
46	Double-shelled hollow microspheres of LiMn2O4 for high-performance lithium ion batteries. Journal of Materials Chemistry, 2011, 21, 9475.	6.7	96
47	Grain Boundary Scattering of Charge Transport in nâ€Type (Hf,Zr)CoSb Halfâ€Heusler Thermoelectric Materials. Advanced Energy Materials, 2019, 9, 1803447.	10.2	88
48	Interrelation between atomic switching disorder and thermoelectric properties of ZrNiSn half-Heusler compounds. CrystEngComm, 2012, 14, 4467.	1.3	87
49	Short-range order in defective half-Heusler thermoelectric crystals. Energy and Environmental Science, 2019, 12, 1568-1574.	15.6	86
50	Halfâ€Heusler Thermoelectric Module with High Conversion Efficiency and High Power Density. Advanced Energy Materials, 2020, 10, 2000888.	10.2	85
51	SnTe–AgSbTe ₂ Thermoelectric Alloys. Advanced Energy Materials, 2012, 2, 58-62.	10.2	78
52	Facile one-pot synthesis of ultrathin NiS nanosheets anchored on graphene and the improved electrochemical Li-storage properties. RSC Advances, 2013, 3, 3899.	1.7	78
53	Enhancing room temperature thermoelectric performance of n -type polycrystalline bismuth-telluride-based alloys via Ag doping and hot deformation. Materials Today Physics, 2017, 2, 62-68.	2.9	76
54	Significant Roles of Intrinsic Point Defects in Mg ₂ <i>X</i> (<i>X</i> = Si, Ge, Sn) Thermoelectric Materials. Advanced Electronic Materials, 2016, 2, 1500284.	2.6	75

#	Article	IF	CITATIONS
55	Enhancing Thermoelectric Performance of n-Type Hot Deformed Bismuth-Telluride-Based Solid Solutions by Nonstoichiometry-Mediated Intrinsic Point Defects. ACS Applied Materials & Interfaces, 2017, 9, 28577-28585.	4.0	71
56	Liquidâ€Phase Hot Deformation to Enhance Thermoelectric Performance of nâ€type Bismuthâ€Tellurideâ€Based Solid Solutions. Advanced Science, 2019, 6, 1901702.	5.6	71
57	Tips-Bundled Pt/Co ₃ O ₄ Nanowires with Directed Peripheral Growth of Li ₂ O ₂ as Efficient Binder/Carbon-Free Catalytic Cathode for Lithium–Oxygen Battery. ACS Catalysis, 2015, 5, 241-245.	5.5	69
58	Demonstration of valley anisotropy utilized to enhance the thermoelectric power factor. Nature Communications, 2021, 12, 5408.	5.8	66
59	loffe–Regel limit and lattice thermal conductivity reduction of high performance (AgSbTe ₂) ₁₅ (GeTe) ₈₅ thermoelectric materials. Journal of Materials Chemistry A, 2014, 2, 3251-3256.	5.2	64
60	High performance n-type bismuth telluride based alloys for mid-temperature power generation. Journal of Materials Chemistry C, 2015, 3, 10597-10603.	2.7	64
61	Transport mechanisms and property optimization of p-type (Zr, Hf)CoSb half-Heusler thermoelectric materials. Materials Today Physics, 2018, 7, 69-76.	2.9	63
62	High-Performance Mg ₃ Sb _{2- <i>x</i>} Bi <i> _x </i> Thermoelectrics: Progress and Perspective. Research, 2020, 2020, 1934848.	2.8	63
63	Self-assembly of a ZnFe2O4/graphene hybrid and its application as a high-performance anode material for Li-ion batteries. New Journal of Chemistry, 2012, 36, 2236.	1.4	62
64	Controllable Synthesis and Shape Evolution of PbTe Three-Dimensional Hierarchical Superstructures via an Alkaline Hydrothermal Method. Journal of Physical Chemistry C, 2009, 113, 8085-8091.	1.5	61
65	Anisotropic thermoelectric properties of layered compound SnSe 2. Science Bulletin, 2017, 62, 1663-1668.	4.3	60
66	Growth and transport properties of Mg3X2 (XÂ= Sb, Bi) single crystals. Materials Today Physics, 2018, 7, 61-68.	2.9	60
67	Half-Heusler thermoelectric materials. Applied Physics Letters, 2021, 118, .	1.5	60
68	Reduced Grain Size and Improved Thermoelectric Properties of Melt Spun (Hf,Zr)NiSn Half-Heusler Alloys. Journal of Electronic Materials, 2010, 39, 2008-2012.	1.0	58
69	Controllable synthesis of high-performance LiMnPO ₄ nanocrystals by a facile one-spot solvothermal process. Journal of Materials Chemistry A, 2014, 2, 10581-10588.	5.2	58
70	Electron and phonon transport in Co-doped FeV0.6Nb0.4Sb half-Heusler thermoelectric materials. Journal of Applied Physics, 2013, 114, 134905.	1.1	54
71	Enhancing thermoelectric performance of FeNbSb half-Heusler compound by Hf-Ti dual-doping. Energy Storage Materials, 2018, 10, 69-74.	9.5	53
72	Evolution of the Intrinsic Point Defects in Bismuth Telluride-Based Thermoelectric Materials. ACS Applied Materials & Interfaces, 2019, 11, 41424-41431.	4.0	53

#	Article	IF	CITATIONS
73	Approaching the minimum lattice thermal conductivity of p-type SnTe thermoelectric materials by Sb and Mg alloying. Science Bulletin, 2019, 64, 1024-1030.	4.3	53
74	Graphene-like δ-MnO ₂ decorated with ultrafine CeO ₂ as a highly efficient catalyst for long-life lithium–oxygen batteries. Journal of Materials Chemistry A, 2017, 5, 6747-6755.	5.2	51
75	Revealing the Intrinsic Electronic Structure of 3D Halfâ€Heusler Thermoelectric Materials by Angleâ€Resolved Photoemission Spectroscopy. Advanced Science, 2020, 7, 1902409.	5.6	49
76	Mushroom-like Au/NiCo ₂ O ₄ nanohybrids as high-performance binder-free catalytic cathodes for lithium–oxygen batteries. Journal of Materials Chemistry A, 2015, 3, 5714-5721.	5.2	48
77	Potassium manganese hexacyanoferrate/graphene as a high-performance cathode for potassium-ion batteries. New Journal of Chemistry, 2019, 43, 11618-11625.	1.4	48
78	Tuning Optimum Temperature Range of Bi ₂ Te ₃ â€Based Thermoelectric Materials by Defect Engineering. Chemistry - an Asian Journal, 2020, 15, 2775-2792.	1.7	46
79	Auâ€Decorated Cracked Carbon Tube Arrays as Binderâ€Free Catalytic Cathode Enabling Guided Li ₂ O ₂ Inner Growth for Highâ€Performance Liâ€O ₂ Batteries. Advanced Functional Materials, 2016, 26, 7725-7732.	7.8	45
80	Enhanced thermoelectric performance in the n-type NbFeSb half-Heusler compound with heavy element Ir doping. Materials Today Physics, 2019, 8, 62-70.	2.9	44
81	Thermoelectric properties of n-type half-Heusler NbCoSn with heavy-element Pt substitution. Journal of Materials Chemistry A, 2020, 8, 14822-14828.	5.2	44
82	Miscibility gap and thermoelectric properties of ecofriendly Mg ₂ Si _{1â^'<i>x</i>} Sn <i>_x</i> (0.1 ≤i>x ≤0.8) solid solutions by flux method. Journal of Materials Research, 2011, 26, 3038-3043.	1.2	42
83	Understanding Moisture and Carbon Dioxide Involved Interfacial Reactions on Electrochemical Performance of Lithium–Air Batteries Catalyzed by Gold/Manganese-Dioxide. ACS Applied Materials & Interfaces, 2015, 7, 23876-23884.	4.0	42
84	Band Structures and Transport Properties of High-Performance Half-Heusler Thermoelectric Materials by First Principles. Materials, 2018, 11, 847.	1.3	42
85	One-pot synthesis of ultrafine ZnFe2O4 nanocrystals anchored on graphene for high-performance Li and Li-ion batteries. RSC Advances, 2014, 4, 7703.	1.7	41
86	Enhanced thermoelectric performance of n-type bismuth-telluride-based alloys via In alloying and hot deformation for mid-temperature power generation. Journal of Materiomics, 2018, 4, 208-214.	2.8	39
87	The Role of Electron–Phonon Interaction in Heavily Doped Fineâ€Grained Bulk Silicons as Thermoelectric Materials. Advanced Electronic Materials, 2016, 2, 1600171.	2.6	38
88	Low Contact Resistivity and Interfacial Behavior of p-Type NbFeSb/Mo Thermoelectric Junction. ACS Applied Materials & Interfaces, 2019, 11, 14182-14190.	4.0	37
89	Thermoelectric performance of p-type zone-melted Se-doped Bi0.5Sb1.5Te3 alloys. Rare Metals, 2018, 37, 308-315.	3.6	36
90	Evolution of nanodomains during the electric-field-induced relaxor to normal ferroelectric phase transition in a Sc-doped Pb(Mg1â^•3Nb2â^•3)O3 ceramic. Journal of Applied Physics, 2007, 102, 084101.	1.1	35

#	Article	IF	CITATIONS
91	Facile solvothermal synthesis of ultrathin LiFe _x Mn _{1â^x} PO ₄ nanoplates as advanced cathodes with long cycle life and superior rate capability. Journal of Materials Chemistry A, 2015, 3, 19368-19375.	5.2	35
92	Facile synthesis of ultrafine CoSn ₂ nanocrystals anchored on graphene by one-pot route and the improved electrochemical Li-storage properties. New Journal of Chemistry, 2013, 37, 474-480.	1.4	34
93	Enhanced thermoelectric performance of Bi2Se3/TiO2 composite. Rare Metals, 2020, 39, 887-894.	3.6	33
94	Self-Assembly of Bi2Te3-Nanoplate/Graphene-Nanosheet Hybrid by One-Pot Route and Its Improved Li-Storage Properties. Materials, 2012, 5, 1275-1284.	1.3	32
95	Increased electrical conductivity in fine-grained (Zr,Hf)NiSn based thermoelectric materials with nanoscale precipitates. Applied Physics Letters, 2012, 100, .	1.5	32
96	Scalable preparation of silicon@graphite/carbon microspheres as high-performance lithium-ion battery anode materials. RSC Advances, 2016, 6, 69882-69888.	1.7	32
97	High performance half-Heusler thermoelectric materials with refined grains and nanoscale precipitates. Journal of Materials Research, 2012, 27, 2457-2465.	1.2	29
98	Elaborating the Crystal Structures of MgAgSb Thermoelectric Compound: Polymorphs and Atomic Disorders. Chemistry of Materials, 2017, 29, 6378-6388.	3.2	29
99	Tunable Optimum Temperature Range of High-Performance Zone Melted Bismuth-Telluride-Based Solid Solutions. Crystal Growth and Design, 2018, 18, 4646-4652.	1.4	29
100	From graphite oxide to nitrogen and sulfur co-doped few-layered graphene by a green reduction route via Chinese medicinal herbs. RSC Advances, 2014, 4, 17902.	1.7	28
101	Bulk Nanostructured Thermoelectric Materials: Preparation, Structure and Properties. Journal of Electronic Materials, 2010, 39, 1990-1995.	1.0	26
102	Oleic acid-assisted preparation of LiMnPO4 and its improved electrochemical performance by Co doping. Journal of Solid State Electrochemistry, 2012, 16, 1271-1277.	1.2	26
103	Controlled Growth of Li ₂ O ₂ by Cocatalysis of Mobile Pd and Co ₃ O ₄ Nanowire Arrays for High-Performance Li–O ₂ Batteries. ACS Applied Materials & Interfaces, 2016, 8, 31653-31660.	4.0	26
104	<i>A</i> ₁₄ MgBi ₁₁ (<i>A</i> = Ca, Sr, Eu): Magnesium Bismuth Based Zintl Phases as Potential Thermoelectric Materials. Inorganic Chemistry, 2017, 56, 10576-10583.	1.9	26
105	Enhancing the average thermoelectric figure of merit of elemental Te by suppressing grain boundary scattering. Journal of Materials Chemistry A, 2020, 8, 8455-8461.	5.2	26
106	Controlled synthesis of nanosized Si by magnesiothermic reduction from diatomite as anode material for Li-ion batteries. International Journal of Minerals, Metallurgy and Materials, 2020, 27, 515-525.	2.4	26
107	Are Solid Solutions Better in FeNbSbâ€Based Thermoelectrics?. Advanced Electronic Materials, 2016, 2, 1600394.	2.6	25
108	Structure, Magnetism, and Thermoelectric Properties of Magnesium-Containing Antimonide Zintl Phases Sr ₁₄ MgSb ₁₁ and Eu ₁₄ MgSb ₁₁ . Inorganic Chemistry, 2017, 56, 1646-1654.	1.9	24

#	Article	IF	CITATIONS
109	Manganese hexacyanoferrate/graphene cathodes for sodium-ion batteries with superior rate capability and ultralong cycle life. Inorganic Chemistry Frontiers, 2018, 5, 2914-2920.	3.0	24
110	Stable cycling of a Prussian blue-based Na/Zn hybrid battery in aqueous electrolyte with a wide electrochemical window. New Journal of Chemistry, 2020, 44, 4639-4646.	1.4	24
111	Ni ₃ S ₂ nanosheet-anchored carbon submicron tube arrays as high-performance binder-free anodes for Na-ion batteries. Inorganic Chemistry Frontiers, 2017, 4, 131-138.	3.0	22
112	Co(OH)2/graphene sheet-on-sheet hybrid as high-performance electrochemical pseudocapacitor electrodes. Journal of Solid State Electrochemistry, 2013, 17, 1159-1165.	1.2	21
113	NiCo ₂ O ₄ /MnO ₂ core/shell arrays as a binder-free catalytic cathode for high-performance lithium–oxygen cells. Inorganic Chemistry Frontiers, 2018, 5, 1707-1713.	3.0	21
114	A new defective 19-electron TiPtSb half-Heusler thermoelectric compound with heavy band and low lattice thermal conductivity. Materials Today Physics, 2020, 13, 100200.	2.9	21
115	Long-life Na-rich nickel hexacyanoferrate capable of working under stringent conditions. Journal of Materials Chemistry A, 2021, 9, 21228-21240.	5.2	21
116	Thermoelectric Properties and n- to p-Type Conversion of Co-Doped ZrNiSn-Based Half-Heusler Alloys. Journal of Electronic Materials, 2012, 41, 1826-1830.	1.0	20
117	The effect of texture degree on the anisotropic thermoelectric properties of (Bi,Sb) ₂ (Te,Se) ₃ based solid solutions. RSC Advances, 2016, 6, 98646-98651.	1.7	20
118	Ru-decorated knitted Co ₃ O ₄ nanowires as a robust carbon/binder-free catalytic cathode for lithium–oxygen batteries. New Journal of Chemistry, 2016, 40, 6812-6818.	1.4	20
119	Synthesis and thermoelectric properties of Rashba semiconductor BiTeBr with intensive texture. Rare Metals, 2018, 37, 274-281.	3.6	20
120	Defect modulation on CaZn _{1â^'x} Ag _{1â^'y} Sb (0 < <i>x</i> < 1; 0 < <i>y</i>) Tj ET Materials Chemistry A, 2018, 6, 11773-11782.	Qq0 0 0 rg 5.2	gBT /Overlock 20
121	Low-cost p-type Bi2Te2.7Se0.3 zone-melted thermoelectric materials for solid-state refrigeration. Journal of Alloys and Compounds, 2020, 831, 154732.	2.8	20
122	Fabrication and thermoelectric properties of Yb-doped ZrNiSn half-Heusler alloys. International Journal of Smart and Nano Materials, 2012, 3, 64-71.	2.0	19
123	Optimum Composition of CaO-SiO2-Al2O3-MgO Slag for Spring Steel Deoxidized by Si and Mn in Production. Metallurgical and Materials Transactions B: Process Metallurgy and Materials Processing Science, 2016, 47, 1435-1444.	1.0	19
124	Enhancing the room temperature thermoelectric performance of n-type Bismuth-telluride-based polycrystalline materials by low-angle grain boundaries. Materials Today Physics, 2022, 22, 100573.	2.9	19
125	Electrochemical performance of Li4Ti5O12/carbon nanofibers composite prepared by an in situ route for Li-ion batteries. Journal of Solid State Electrochemistry, 2012, 16, 3915-3921.	1.2	17
126	Mo-Fe/NbFeSb Thermoelectric Junctions: Anti-Thermal Aging Interface and Low Contact Resistivity. ACS Applied Materials & Interfaces, 2021, 13, 7317-7323.	4.0	17

#	Article	IF	CITATIONS
127	Microstructure and thermoelectric properties of InSb compound with nonsoluble NiSb in situ precipitates. Journal of Materials Research, 2013, 28, 3394-3400.	1.2	16
128	Multiscale Defects as Strong Phonon Scatters to Enhance Thermoelectric Performance in Mg ₂ Sn _{1–} <i>_x</i> Sb <i>_x</i> Solid Solutions. Small Methods, 2019, 3, 1900412.	4.6	16
129	Electrochemical Compatibility of Solidâ€&tate Electrolytes with Cathodes and Anodes for Allâ€&olidâ€&tate Lithium Batteries: A Review. Advanced Energy and Sustainability Research, 2021, 2, 2000101.	2.8	16
130	In situ transmission electron microscopy study of the nanodomain growth in a Sc-doped lead magnesium niobate ceramic. Applied Physics Letters, 2006, 89, 022904.	1.5	15
131	Modulating the resistivity of MoS2 through low energy phosphorus plasma implantation. Applied Physics Letters, 2017, 110, .	1.5	15
132	High-Power-Density Wearable Thermoelectric Generators for Human Body Heat Harvesting. ACS Applied Materials & Interfaces, 2022, 14, 21224-21231.	4.0	15
133	Controllable synthesis of hollow α-Fe2O3 nanostructures, their growth mechanism, and the morphology-reserved conversion to magnetic Fe3O4/C nanocomposites. RSC Advances, 2013, 3, 19097.	1.7	14
134	Trace fluorinated-carbon-nanotube-induced lithium dendrite elimination for high-performance lithium–oxygen cells. Nanoscale, 2020, 12, 3424-3434.	2.8	14
135	Structure and properties of (1 â^' x)Pb(Mg1/2W1/2)O3 â^' xPb(Zr0.5Ti0.5)O3 solid solution ceramics. Journal of Materials Science, 2008, 43, 5258-5264.	1.7	13
136	Grain size effect on the phase transformations of higher manganese silicide thermoelectric materials: An in situ energy dispersive x-ray diffraction study. Journal of Materials Research, 2011, 26, 1900-1906.	1.2	13
137	Ordered LiMPO4 (M = Fe, Mn) nanorods synthesized from NH4MPO4·H2O microplates by stress involved ion exchange for Li-ion batteries. CrystEngComm, 2014, 16, 2239.	1.3	13
138	Carboxymethyl cellulose and composite films prepared by electrophoretic deposition and liquid-liquid particle extraction. Colloid and Polymer Science, 2018, 296, 927-934.	1.0	13
139	Scattering Mechanisms and Compositional Optimization of Highâ€Performance Elemental Te as a Thermoelectric Material. Advanced Electronic Materials, 2020, 6, 2000038.	2.6	13
140	Scale-up processing of a safe quasi-solid-state lithium battery by cathode-supported solid electrolyte coating. Materials Today Energy, 2021, 21, 100841.	2.5	13
141	MICROSTRUCTURE AND THERMOELECTRIC PROPERTIES OF (Zr,Hf)NiSn-BASED HALF-HEUSLER ALLOYS BY MELT SPINNING AND SPARK PLASMA SINTERING. Functional Materials Letters, 2010, 03, 227-231.	0.7	12
142	Electrochemical performance of TiO ₂ /carbon nanotubes nanocomposite prepared by an in situ route for Li-ion batteries. Journal of Materials Research, 2012, 27, 417-423.	1.2	12
143	Reduced graphene oxide induced confined growth of PbTe crystals and enhanced electrochemical Li-storage properties. RSC Advances, 2013, 3, 23612.	1.7	12
144	Synthesis and liquid-liquid extraction of non-agglomerated Al(OH)3 particles for deposition of cellulose matrix composite films. Journal of Colloid and Interface Science, 2017, 508, 49-55.	5.0	12

#	Article	IF	CITATIONS
145	Enhancing room-temperature thermoelectric performance of n-type Bi2Te3-based alloys via sulfur alloying. Rare Metals, 2021, 40, 513-520.	3.6	12
146	Graphene-induced confined crystal growth of octahedral Zn ₂ SnO ₄ and its improved Li-storage properties. Journal of Materials Research, 2012, 27, 3096-3102.	1.2	11
147	Reliable measurements of the Seebeck coefficient on a commercial system. Journal of Materials Research, 2015, 30, 2670-2677.	1.2	11
148	Lithiated carbon cloth as a dendrite-free anode for high-performance lithium batteries. Sustainable Energy and Fuels, 2020, 4, 5773-5782.	2.5	11
149	Multiwalled carbon nanotubes mass-produced by dc arc discharge in He–H2 gas mixture. Journal of Nanoparticle Research, 2006, 8, 279-285.	0.8	10
150	Influence of NaOH on the synthesis of Bi2Te3 via a low-temperature aqueous chemical method. Journal of Materials Science, 2009, 44, 3528-3532.	1.7	10
151	Synthesis and electrochemical performance of YF3-coated LiMn2O4 cathode materials for Li-ion batteries. Rare Metals, 2011, 30, 39-43.	3.6	10
152	First-principles studies of lattice dynamics and thermal properties of Mg ₂ Si _{1â^'<i>x</i>} Sn _{<i>x</i>} . Journal of Materials Research, 2015, 30, 2578-2584.	1.2	10
153	Architecture-independent reactivity tuning of Ni/Al multilayers by solid solution alloying. Applied Physics Letters, 2019, 114, 183102.	1.5	10
154	Morphology of graphite in hot-compressed nodular iron. Journal of Materials Science, 2004, 39, 6093-6096.	1.7	9
155	Doping effect on thermoelectric properties of nonstoichiometric AgSbTe2 compounds. International Journal of Minerals, Metallurgy and Materials, 2011, 18, 352-356.	2.4	9
156	Hot deformation induced defects and performance enhancement in FeSb2 thermoelectric materials. Journal of Applied Physics, 2013, 114, .	1.1	9
157	Hollow nano silicon prepared by a controlled template direction and magnesiothermic reduction reaction as anode for lithium ion batteries. New Journal of Chemistry, 2014, 38, 4177.	1.4	9
158	In situ synthesis of silver/chemically reduced graphene nanocomposite and its use for low temperature conductive paste. Journal of Materials Science: Materials in Electronics, 2017, 28, 7686-7691.	1.1	9
159	Electrochemical properties of Zn4Sb3 as anode materials for lithium-ion batteries. Journal of Materials Science Letters, 2000, 19, 851-853.	0.5	8
160	Glass-forming ability and I-phase formation in Y-doped Zr–Nb–Cu–Ni–Al glassy alloys. Philosophical Magazine Letters, 2009, 89, 11-18.	0.5	8
161	Electrochemical performance of LiMn2O4 microcubes prepared by a self-templating route. Journal of Solid State Electrochemistry, 2013, 17, 2589-2594.	1.2	8
162	Facile synthesis of nanostructured LiMnPO ₄ as a high-performance cathode material with long cycle life and superior rate capability. RSC Advances, 2015, 5, 99632-99639.	1.7	8

#	Article	IF	CITATIONS
163	Forging Inspired Processing of Sodiumâ€Fluorinated Graphene Composite as Dendriteâ€Free Anode for Longâ€Life Na–CO ₂ Cells. Energy and Environmental Materials, 2022, 5, 572-581.	7.3	8
164	Low-cost and scalable preparation of nano-Si from photovoltaic waste silicon for high-performance Li-ion battery anode. Functional Materials Letters, 2021, 14, 2151033.	0.7	8
165	Preparation and Li-storage properties of SnSb/graphene hybrid nanostructure by a facile one-step solvothermal route. International Journal of Smart and Nano Materials, 0, , 1-11.	2.0	7
166	LiMn ₂ O ₄ microspheres secondary structure of nanoparticles/plates as cathodes for Li-ion batteries. Journal of Materials Research, 2013, 28, 1343-1348.	1.2	7
167	Anisotropic Thermoelectric Properties of <i>n</i> -Type Te-Free (Bi, Sb) ₂ Se ₃ with Orthorhombic Structure. ACS Applied Energy Materials, 2020, 3, 2070-2077.	2.5	7
168	Unexpected Low-Temperature Performance of Li–O ₂ Cells with Inhibited Side Reactions. ACS Applied Materials & Interfaces, 2018, 10, 25925-25929.	4.0	6
169	Influence of Electron–Phonon Interaction on the Lattice Thermal Conductivity in Singleâ€Crystal Si. Annalen Der Physik, 2020, 532, 1900435.	0.9	6
170	Additive-aided electrochemical deposition of bismuth telluride in a basic electrolyte. International Journal of Minerals, Metallurgy and Materials, 2010, 17, 489-493.	2.4	5
171	Thermoelectric properties of Sb-doped Mg ₂ Si _{0.59} Sn _{0.41} solid solutions. Physica Status Solidi (A) Applications and Materials Science, 2013, 210, 2359-2363.	0.8	5
172	Superamphiphobic Porous Structure: Design and Implementation. Advanced Materials Interfaces, 2019, 6, 1801973.	1.9	5
173	Low interfacial resistivity in CoSi2/ZrCoSb thermoelectric junctions. Materials Today Energy, 2022, 25, 100960.	2.5	5
174	Pr-doping effect on the depinning of vortices in Bi2Sr2Ca1â^'xPrxCu2Oy single crystals. Journal of Applied Physics, 2000, 87, 5567-5569.	1.1	4
175	Tube encapsulation effects in various carbon nanotube systems. Physica Status Solidi (B): Basic Research, 2007, 244, 4082-4085.	0.7	4
176	One-pot synthesis of core–shell structured Sn/carbon nanotube by chemical vapor deposition and its Li-storage properties. Journal of Materials Research, 2011, 26, 2719-2724.	1.2	4
177	Defect control in Ca _{1â^{~°}δ} Ce _δ Ag _{1â^{~°}δ} Sb (δ â‰^ 0.15) through Nb doping. Inorganic Chemistry Frontiers, 2017, 4, 1113-1119.	3.0	4
178	lonic liquid/ether-plasticized quasi-solid-state electrolytes for long-life lithium–oxygen cells. New Journal of Chemistry, 2018, 42, 19521-19527.	1.4	4
179	Electrochemical lithium intercalation in CoSb3 compound. Journal of Materials Science Letters, 2003, 22, 221-224.	0.5	3
180	Preparation and properties of antimony thin film anode materials. Science Bulletin, 2004, 49, 1882-1885.	1.7	3

#	Article	IF	CITATIONS
181	Hydrogen storage properties of ball-milled Mg-based composite with PdCl2 additive. Journal of Zhejiang University: Science A, 2007, 8, 1510-1513.	1.3	3
182	P-type doping of Hf0.6Zr0.4NiSn half-Heusler thermoelectric materials prepared by levitation melting and spark plasma sintering. Journal of Materials Research, 2011, 26, 1913-1918.	1.2	3
183	Tiny amounts of fluorinated carbon nanotubes remove sodium dendrites for high-performance sodium–oxygen batteries. Sustainable Energy and Fuels, 2020, 4, 4108-4116.	2.5	3
184	Enhanced cycle stability of spinel LiMn2O4 by a melting impregnation method. Frontiers of Materials Science in China, 2008, 2, 291-294.	0.5	2
185	Enhanced thermoelectric properties of Co1â~'xâ~'y Ni x+y Sb3â~'x Sn x materials. International Journal of Minerals, Metallurgy and Materials, 2012, 19, 240-244.	2.4	2
186	One-pot synthesis of Sb-Fe-carbon-fiber composites with in situ catalytic growth of carbon fibers. International Journal of Minerals, Metallurgy and Materials, 2012, 19, 542-548.	2.4	2
187	Nonequivalence of the anisotropy in the normal state to that in the superconducting state ofBi2Sr2Ca(Cu1â^'xMx)2Oy(M=Mn,Fe, Co, and Ni). Physical Review B, 2000, 62, 11384-11387.	1.1	1
188	Electrochemical properties of CoFe3Sb12 as potential anode material for lithium-ion batteries. Journal of Zhejiang University: Science A, 2004, 5, 418-421.	1.3	1
189	Nanostructured Bi2Te3 synthesized by low temperature aqueous chemical route. Frontiers of Chemistry in China: Selected Publications From Chinese Universities, 2006, 1, 188-192.	0.4	1
190	Long Rang Cation Order in Pb(Mg <inf>1/3</inf> Nb <inf>2/3</inf>)O <inf>3</inf> Complex Oxides. Applications of Ferroelectrics, IEEE International Symposium on, 2007, , .	0.0	1
191	Solvothermal synthesis and thermoelectric properties of skutterudite compound Fe0.25Ni0.25Co0.5Sb3. Rare Metals, 2009, 28, 237-240.	3.6	1
192	Controllable synthesis of PbTe nanosheets via an alkaline hydrothermal method. , 2010, , .		1
193	Effect of PbTe on Thermoelectric Properties of Co0.88Ni0.12Sb2.91Sn0.09. Journal of Inorganic and Organometallic Polymers and Materials, 2011, 21, 862-865.	1.9	1
194	Electrochemical kinetics of nanosized Ag and Ag2O thin films prepared by radio frequency magnetron sputtering. Journal of Solid State Electrochemistry, 2011, 15, 2031-2039.	1.2	1
195	Preparation of silver/chemically reduced graphene composite for flexible printed circuits. Micro and Nano Letters, 2018, 13, 576-579.	0.6	1
196	Cation and dipole order in ferroelectric perovskite oxides. , 2008, , .		0
197	SELF-ASSEMBLY OF BISMUTH SELENIDE TWO-DIMENSIONAL SUPERSTRUCTURE FROM HEXAGONAL NANOSHEETS. Functional Materials Letters, 2011, 04, 245-248.	0.7	0
198	RAPID SYNTHESIS OF CoSb3/GRAPHENE NANOCOMPOSITES BY ONE-POT SOLVOTHERMAL ROUTE AND THEIR ELECTROCHEMICAL PROPERTIES. Functional Materials Letters, 2012, 05, 1250002.	0.7	0